Contemporary Engineering Sciences, Vol. 7, 2014, no. 3, 117 - 134
HIKARI Ltd, www.m-hikari.com
http://dx.doi.org/10.12988/ces.2014.31064

A Method for the Detection of Diabetic Retinopathy, by Analyzing the Image of the Retinal Vascular Network

B. Luna-Benoso

Instituto Politécnico Nacional
Escuela Superior de Cómputo
Av. Juan de Dios Batíz, esq. Miguel Othón de Mendizábal
Cuidad de México 07320, México
blunabenoso@yahoo.com

J. C. Martínez Perales

Instituto Politécnico Nacional
Escuela Superior de Cómputo
Av. Juan de Dios Batíz, esq. Miguel Othón de Mendizábal
Cuidad de México 07320, México
pepe_cruzm@hotmail.com

R. Flores-Carapia

Instituto Politécnico Nacional
Centro de Innovación y Desarrollo Tecnológico en Cómputo
Av. Juan de Dios Batíz, esq. Miguel Othón de Mendizábal
Ciudad de México 07700, México
rfcarapia@yahoo.com

A. L. Barrales López

Instituto Politécnico Nacional
Centro de Innovación y Desarrollo Tecnológico en Cómputo
Av. Juan de Dios Batíz, esq. Miguel Othón de Mendizábal
Ciudad de México 07700, México

Abstract

Diabetic retinopathy is a complication of diabetes caused by changes in the blood vessels of the retina, can cause blindness if not detected and treated early. Exudates and hemorrhages are two major signs present in diabetic retinopathy. This paper presents an automated method for classifying patients suffering from diabetic retinopathy by analyzing the image of the retinal vascular network. The proposed method is divided into three stages: segmentation of hemorrhages and exudates by digital image processing of retinal vascular network using spatial domain methods, extraction of characteristics using Hu moments, and pattern recognition by using associative memories based on cellular automata.

Keywords: Digital Imaging, Hu invariant moments, associative memories, hemorrhages, exudates

1. Introduction

Diabetes is a disease that occurs when the pancreas does not secrete enough insulin or the body is unable to process it properly. This disease affects the circulatory system slowly including the retina. As diabetes progresses, the vision of a patient may begin to deteriorate and lead to diabetic retinopathy. Diabetic retinopathy is a condition due to prolonged exposure of diabetes that damages the eye and can lead to the total loss [8]. Diabetic retinopathy is difficult to diagnose when it is in its first stage known as proliferative diabetic retinopathy, which is characterized by microaneurysms, exudates and hemorrhages [[2], [4]]. Microaneurysms are small protruding arterial dilation of capillaries, one of the earliest detectable clinical signs of diabetic retinopathy [[9]]. The exudates consist of fat deposited in the nerve fiber layer of the retina, and are presented in rounded or oval formations, yellowish-white indistinct borders [[16]]. Bleeding is the bleeding of blood vessels as a result of weakened hair breakage [[6]].
This paper presents an automated method for the detection of diabetic retinopathy from images of the retinal vascular network. The method is divided into three stages: 1) segmentation of hemorrhages and exudates using spatial domain methods, 2) feature extraction using Hu moments, and 3) classification by using associative memories based on cellular automata.

2. Spatial domain methods

A digital image is a two-dimensional function $f(x, y)$ of the light intensity (brightness) at a point in space, where (x, y) coordinates of that point. Since a digital image is a function $f(x, y)$ discretized in both spatial coordinates and in brightness, often commonly represented as a two dimensional matrix $F_{ij} = (f_{ij})m \times n$, where m and n represent the image size and $f_{ij} = f(x_i, x_j)$. Each element of the array is called picture element or pixel. The spatial domain refers to the image plane itself, and techniques in this category are based on the direct manipulation of the pixels in the image [[11]] (Figure 1).

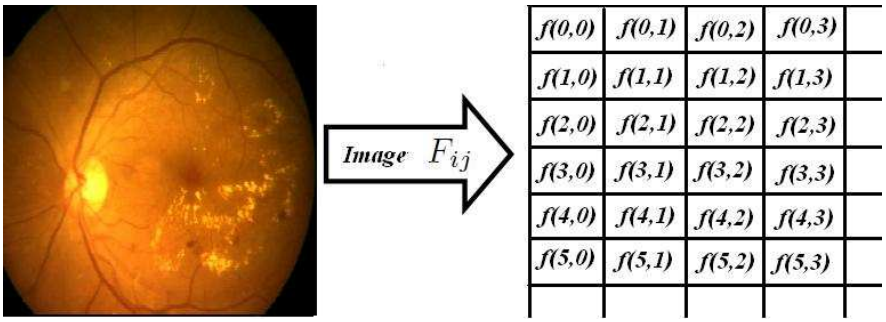

Figure 1: Digital image.

3. Hu Moments

Hu moments are numerical properties can be obtained from a certain image from the pixels that compose it. Hu moments are invariant with respect to translations, rotations and scalings. To define Hu moments, consider the following previous definitions [[11], [7]].

Statistical moments are defined as $m_{rs} = \sum_{i,j \in REG} i^r j^s$, where $r, s \in \mathbb{N}$ y REG the set of pixels within the region.

The center of gravity of a region defined by the coordinates $(\overline{i}, \overline{j})$ where $\overline{i} = \frac{m_{10}}{m_{00}}$ and $\overline{j} = \frac{m_{01}}{m_{00}}$.

From the center of gravity, central moments are defined as $\mu_{rs} = \sum_{i,j \in REG} (i - \overline{i})^r (j - \overline{j})^s$.

From the previous concepts, are defined 7 Hu moments as follows:
$\Phi_1 = \eta_{20} + \eta_{02}$
$\Phi_2 = (\eta_{20} - \eta_{02})^2 + 4\eta_{11}^2$
$\Phi_3 = (\eta_{30} - 3\eta_{12})^2 + (3\eta_{21} - \eta_{03})^2$
$\Phi_4 = (\eta_{30} + \eta_{12})^2 + (\eta_{21} + \eta_{03})^2$
$\Phi_5 = (\eta_{30} - 3\eta_{12})(\eta_{30} + \eta_{12})[(\eta_{30} + \eta_{12})^2 - 3(\eta_{21} + \eta_{03})^2] + (3\eta_{21} - \eta_{03})(\eta_{21} + \eta_{03})[3(\eta_{30} + \eta_{12})^2 - (\eta_{21} + \eta_{03})^2]$
$\Phi_6 = (\eta_{20} - \eta_{02})[(\eta_{30} + \eta_{12})^2 - (\eta_{21} + \eta_{03})^2] + 4\eta_{11}(\eta_{30} + \eta_{12})(\eta_{21} + \eta_{03})$
$\Phi_7 = (3\eta_{21} - \eta_{03})(\eta_{30} + \eta_{12})[(\eta_{30} + \eta_{12})^2 - 3(\eta_{21} + \eta_{03})^2] - (\eta_{30} - 3\eta_{12})(\eta_{21} + \eta_{03})[3(\eta_{30} + \eta_{12})^2 - (\eta_{21} + \eta_{03})^2]$

Where

$$\eta_{rs} = \frac{\mu_{rs}}{\mu_{00}^t} \text{ and } t = \frac{r+s}{2} + 1.$$

4. Associative Memories

Associative memories are mathematical models whose main objective is to recover complete patterns from input patterns. The operation of the associative memory is divided into two phases: learning stage where the associative memory is generated, and phase recovery stage where the associative memory operates [[13], [17]].

During the learning phase, the associative memory is constructed from a set of ordered pairs of patterns known in advance, called fundamental set. Each pattern that defines the fundamental set are called fundamental pattern. The fundamental set is represented as follows [[1]]:

$$FS = \{(\mathbf{x}^\mu, \mathbf{y}^\mu) | \mu = 1, 2, \ldots, p\} \tag{1}$$

where $(\mathbf{x}^\mu, \mathbf{y}^\mu) \in A^n \times A^m$ for $\mu = 1, 2, \ldots, p$, with $A = \{0, 1\}$.

During the recovery phase, the associative memory operating with an input pattern for the corresponding output pattern.

5. Cellular Automata

Let I be a set of indices. Let $A = \{[a_i, b_i]\}_{i \in I}$ countable family of closed intervals in $\mathbb{R}$ such that the following conditions:

1. $\bigcup_{X \in A} X = [a, b]$ for some $a, b \in \mathbb{R}$ o $\bigcup_{X \in A} X = \mathbb{R}$.
2. if $[a_i, b_i] \in A$, then $b_i - a_i > 0$.
3. if $[a_i, b_i]$ and $[c_j, d_j]$ are in A with $b_i \leq c_j$, then $[a_i, b_i] \cap [c_j, d_j] = \emptyset$ or $[a_i, b_i] \cap [c_j, d_j] = b_i = c_j$.

Definition 5.1 Let $[a, b]$ an interval of $\mathbb{R}$ with $a \neq b$ and A a family of closed intervals that satisfy 1, 2 and 3. A 1-dimensional lattice is the set $\mathcal{L} = \{x_i \times [a, b] \mid x_i \in A\}$. If $A_1, A_2, \ldots, A_n$ are families of intervals that meets 1, 2 and 3, then a lattice of dimension $n > 1$ is the set $\mathcal{L} = \{x_1 \times x_2 \times \cdots \times x_n \mid x_i \in A_i\}$.

Definition 5.2 Let $r \in \mathbb{R}$. An 1-dimensional lattice is regular if $[a_i, b_i] = r$ for each $[a_i, b_i] \in A$. An n-dimensional lattice is *regular* if $[a_{i_k}, b_{i_k}] = r$ for each $[a_{i_k}, b_{i_k}] \in A_i$ for $i = 1, 2, \ldots, n$.

Definition 5.3 Let $\mathcal{L}$ be a lattice. A cell or site is an element of $\mathcal{L}$, that is, a

cell is an element of the form $[a_{1_k}, b_{1_k}] \times \cdots \times [a_{n_k}, b_{n_k}]$ with $[a_{i_k}, b_{i_k}] \in A_i$ for $i = 1, 2, \ldots, n$.

Definition 5.4 Let $\mathcal{L}$ be a lattice, and r is a cell of $\mathcal{L}$. A neighborhood of size $n \in \mathbb{N}$ for r, is the set $v(r) = \{\{k_1, k_2, \ldots, k_n\} | k_j$ is a cell of $\mathcal{L}$ for each $j\}$.

Definition 5.5 Let $n \in \mathbb{N}$. A cellular automaton is a tuple $(\mathcal{L}, \mathcal{S}, \mathcal{N}, f)$ such that:

1. $\mathcal{L}$ is a regular lattice.
2. $\mathcal{S}$ is a finite set of states.
3. $\mathcal{N}$ is a set of neighborhoods nest as follows:

$$\mathcal{N} = \{v(r) \mid r \text{ is a cell and } v(r) \text{ is a neighborhood } r \text{ of size } n\}$$

4. $f : \mathcal{N} \to \mathcal{S}$ is a function called the transition function.

Definition 5.6 A configuration of the cellular automaton $(\mathcal{L}, \mathcal{S}, \mathcal{N}, f)$ is a function $C_t : \mathcal{L} \to \mathcal{S}$ which associates to each cell of the lattice $\mathcal{L}$ at time t, a state of $\mathcal{S}$.
If $(\mathcal{L}, \mathcal{S}, \mathcal{N}, f)$ is a cellular automaton and $r \in \mathcal{L}$, then the configuration C_t is related with f through:

$$C_t = f(\{C_t(i) | i \in \mathcal{N}(r)\})$$

Definition 5.7 Let $\mathcal{Q} = (\mathcal{L}, \mathcal{S}, \mathcal{N}, f)$ and $\mathcal{W} = (\mathcal{L}, \mathcal{S}, \mathcal{N}', g)$ two cellular automata. Cellular automaton composition of the CA $\mathcal{Q}$ and $\mathcal{W}$ in the time $t = t_k$ is defined as $\mathcal{W} * \mathcal{Q}$ by the cellular automaton $\mathcal{W} * \mathcal{Q} = (L, S, N, h)$ where h, f and g are related as follows:

$$C_{t_k+1}(r) = f(\{C_{t_k}(i) : i \in \mathcal{N}(r)\}$$

$$C_{t_k+2}(r) = g(\{C_{t_k+1}(i) : i \in \mathcal{N}'(r)\}$$

$$C_{t_k+2}(r) = h(\{C_{t_k}(i) : i \in \mathcal{N}(r)\}$$

Definition 5.8 Let $\mathcal{R} = (\mathcal{L}, S, \mathcal{N}, f)$ a cellular automaton with $\mathcal{L} = \mathbb{Z}^2$. If $A \subseteq \mathbb{Z}^2$ and $x \in S$, then $[A]_x$ denote the number of cells in A with state x.

6. Associative Memories based on Cellular Automata

In this work we used the associative memory model based on cellular automata by the authors in [[10]]. Immediately previous definitions are presented and the proposed model.

Definition 6.1 Are $A, B \subseteq \mathbb{Z}^2$. The cell expansion is the cellular automata $\mathcal{D} = (\mathcal{L}, S, \mathcal{N}, f)$ with initial configuration A, defined as follows:

- $\mathcal{L} = \mathbb{Z}^2$.
- $S = \{0, 1\}$.
- $\mathcal{N} = \{v_x | x \in \mathcal{L}\}$ with $v_x = (B^-)_x = \{-b + x | b \in B\}$.
- The transition function $f : \mathcal{N} \to S$ is given as follows:

$$f(v_x) = \begin{cases} 1 & \text{if} \quad [v_x]_1 > 0 \\ \\ 0 & \text{if} \quad [v_x]_1 = 0 \end{cases}$$

Definition 6.2 Are $A, B \subseteq \mathbb{Z}^2$. Erosion is the cellular automata cell $\mathcal{D} = (\mathcal{L}, S, \mathcal{N}, f)$ with initial configuration A, defined as follows:

- $\mathcal{L} = \mathbb{Z}^2$.
- $S = \{0, 1\}$.
- $\mathcal{N} = \{v_x | x \in \mathcal{L}\}$ with $v_x = (B)_x = \{b + x | b \in B\}$.
- The transition function $f : \mathcal{N} \to S$ is:

$$f(v_x) = \begin{cases} 1 & \text{if} \quad [v_x]_1 = |B| \\ \\ 0 & \text{if} \quad [v_x]_1 < |B| \end{cases}$$

In what follows, consider the set $A = \{0, 1\}$ and the fundamental set $FS = \{(\mathbf{x}^\mu \mathbf{y}^\mu) | \mu = 1, 2, \ldots, p\}$ with $\mathbf{x}^\mu \in A^n$ and $\mathbf{y}^\mu \in A^m$.

The lattice $\mathcal{L}$ for the CA shall consist of the matrix of size $2m \times 2n$ with the first index in $(0, 0)$.

The set $\mathcal{S} = \{0, 1\}$ is the finite set of states.

Let $I = \{i \in \mathbb{Z} | i = 2k \text{ for } k = 0, 1, 2, \ldots, n-1\} = \{0, 2, 4, \ldots, 2(n) - 2\}$ and $J = \{j \in \mathbb{Z} | j = 2k + 1 \text{ for } k = 0, 1, 2, \ldots, m-1\} = \{1, 3, 5, \ldots, 2m - 1\}$. Consider the partition of $\mathcal{L}$ formed by the family of subsets $IJ = \{v_{(i,j)} | (i, j) \in I \times J\}$ with $v_{(i,j)} = \{(i, j), (i, j-1), (i+1, j), (i+1, j-1)\}$. Since IJ is a partition of $\mathcal{L}$, given $\boldsymbol{l} \in \mathcal{L}$, exists a unique $(i, j) \in I \times J$ such that $\boldsymbol{l} \in v_{(i,j)}$. We denote by $v^{\boldsymbol{l}}$ this single element, i.e. $v^{\boldsymbol{l}} = v_{(i,j)}$. For example, if $\boldsymbol{l} = (3, 0)$ then $\boldsymbol{l} \in v^{(3,0)} = v_{(2,1)} = \{(2, 1), (2, 0), (3, 1), (3, 0)\}$.

From the above fact it defines the set of neighborhoods

$$\mathcal{N} = \{v^{\boldsymbol{l}} | \boldsymbol{l} \in \mathcal{L}\} \tag{2}$$

Definition 6.3 Consider the set A^k. We define the projection function of the i-th component $(1 \leq i \leq k)$ as $Pr_i : A^k \to A$ as:

$$Pr_i(\mathbf{z}) = z_i, with\ \mathbf{z} = (z_1, z_2, \ldots, z_k) \tag{3}$$

Theorem 6.4 If $(y_i, x_j) \in Pr_{\mathbf{yx}} = \{(y_i, x_j) | y_i = Pr_i(\mathbf{y})\ and\ x_j = Pr_j(\mathbf{x})\}$, then $(2j - 2 + y_i, 2i - 2 + x_j) \in v_{(2j-2,2i-1)}$. We define the set $\mathcal{L}_{FS} = \{(2j - 2 + y_i^{\mu}, 2i - 2 + x_j^{\mu}) | 1 \leq \mu \leq p, 1 \leq i \leq m\ and\ 1 \leq j \leq n\} \subseteq \mathcal{L}$.

Consider the CA $\mathcal{Q} = (\mathcal{L}, \mathcal{S}, \mathcal{N}, f_{\mathcal{Q}})$ and $\mathcal{W} = (\mathcal{L}, \mathcal{S}, \mathcal{N}', f_{\mathcal{W}})$ with $\mathcal{N}' = IJ$, and $f_{\mathcal{Q}} : \mathcal{N} \to S$, $f_{\mathcal{W}} : \mathcal{N}' \to S$ defined as follows:

$$f_{\mathcal{Q}}(v^{(i,j)}) = \begin{cases} 1 & \text{if} \quad (i, j) \in \mathcal{L}_{FS} \\ \\ 0 & \text{if} \quad (i, j) \notin \mathcal{L}_{FS} \end{cases}$$

$$f_{\mathcal{W}}(v_{(i,j)}) = \begin{cases} 1 & \text{in position } (i+1, j) \quad \text{if } (i, j-1) = 1 \\ \\ 1 & \text{in position } (i, j-1) \quad \text{if } (i+1, j) = 1 \end{cases}$$

We define the Associative CA (ACA) in its learning phase as

$$\mathcal{W} * \mathcal{Q} = (\mathcal{L}, \mathcal{S}, \mathcal{N}, f_A) \tag{4}$$

The recovery phase for the ACA makes use of the composition of erosions and dilations CA. The algorithm which defines the phase of recovery is shown in algorithm 1.

Algorithm 1 *ACA* in recovery phase

Require: Fundamental set $FS = \{(\mathbf{x}^\mu, \mathbf{y}^\mu) | \mu = 1, 2, \ldots, p\}$; structuring element B; integer value ne (number of erosions); integer value nd (number of dilations); pattern to recovery $\tilde{\mathbf{x}} \in A^n$

Ensure: Recovery pattern $\tilde{\mathbf{y}} \in A^m$

1. Building the Learning ACA for FS.
2. Applying ne times the cell erosion $\mathcal{E}$ with the structuring element B to the initial configuration of learning ACA. This is, applied to the configuration of the ACA, $\mathcal{E} * \mathcal{E} * \cdots * \mathcal{E}$, ne times.
3. Applying nd times the cellular dilation with the structuring element $\mathcal{D}$ to configuration obtained in point 2. This is, applied to the configuration obtained in point 2, $\mathcal{D} * \mathcal{D} * \cdots * \mathcal{D}$, nd times.
4. For the input pattern $\tilde{\mathbf{x}} \in An$ will get the output pattern $\tilde{\mathbf{y}} \in A^m$ applying:

for $i = 1 \to m$ **do**
  $\tilde{y}_i = 1$
  for $j = 1 \to n$ **do**
    if $\neg(\tilde{x}_j = 0 \wedge (2j-1, 2i-2) = 1)$ **then**
      if $\neg(\tilde{x}_j = 1 \wedge ((2j-2, 2i-2) = 1 \vee (2j-1, 2i-2) = 1))$ **then**
        $\tilde{y}_i = 0$
        $Break$
      end if
    end if
  end for
end for

7. Proposed method

The method described in this paper is divided into three stages: 1) segmentation of hemorrhages and exudates, 2) feature extraction using Hu moments, and 3) classification by using associative memories.

1) **Segmentation of hemorrhages and exudates.** Figure 2 corresponds to the retinal vascular network of an individual suffering from diabetic retinopathy, it is observed the presence of bleeding and exudates, main characteristics of the disease.

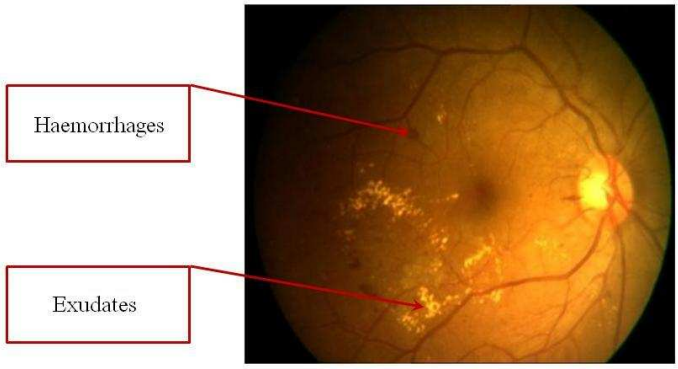

Figure 2: Presence of exudates and hemorrhages in retinal vascular network of an individual suffering from diabetic retinopathy.

In the first stage, the objective is to obtain the segmentation of image bleeding and exudates in retinal vascular network to this end, methods were used in the spatial domain. For obtaining exudates, the method consists of 4 steps: 1. Obtaining the grayscale image 2. Implementation of Laplacian of Gaussian filter, 3. Segmentation threshold binarization with a-b, and 4. Application of median filter.

7.1 Obtaining the grayscale image

A grayscale image is obtained by extracting the green channel from the decomposition of a color image in the three RGB channels [[11]].

7.2 Laplacian of Gaussian filter

The Laplacian of Gaussian filter to detect edges softening the image applying the second derivative of Gaussian filter equation [[14]]. The equation defining the Laplacian when the mask used is shown in Figure 3 is:

$$\nabla^2 f = 4z_5 - (z_2 + z_4 + z_6 + z_8) \tag{5}$$

0	-1	0
-1	4	-1
0	-1	0

Figure 3: Mask to calculate the Laplacian.

7.3 Segmentation by binarization with threshold a-b

It consists of making a journey to the matrix representation of the image and assign a binary value (0 for black and 255 for white) to each pixel depending on the thresholds a and b. If (x, y) represents the coordinates of a pixel $f(x, y)$ the value corresponding grayscale then the binarization by $a - b$ threshold is as follows: [[11]]:

$$f(x,y) = \begin{cases} 0 & \text{if} \quad a \leq f(x,y) \leq b \\ \\ 255 & \text{if} \quad f(x,y) < a \ o \ f(x,y) > b \end{cases} \tag{6}$$

7.4 Median Filter

The median filter replaces each pixel in the image by the median of the pixels in the mask containing the nearest neighbors [[11]]. For example if we consider Figure 4, in order of increasing the pixel values are covered by the mask 115, 119, 120, 123, 124, 125, 126, 127 and 150, where the median value is 124.

124	126	127
120	150	125
115	119	123

→

124	126	127
120	124	125
115	119	123

Figure 4: Median filter.

For obtaining bleeds, the method consists of five steps: 1. Obtaining greyscale image 2. Targeting $a - b$ binarization with threshold 3. Dilation 4. Obtejos removal and 5. Erosion.

Mathematical morphology is a mathematical tool based on set theory and used with great success in the digital processing of binary images [[3]]. The fundamental operations of mathematical morphology are dilation and erosion [[15]].

7.5 Dilation

A and B are two sets, wherein A represents a binary image. A dilation by B,

denoted $A \oplus B$ is defined as: [[12]]

$$A \oplus B = \{a + b | a \in A \; and \; b \in B\} \tag{7}$$

The set B is called structuring element.

7.6 Elimination of objects

To remove large objects are considered connected components of the binary image using 8- connectivity. Taking all connected components of the image eliminates all those that exceed a certain threshold, ie, for this step, we applied the following formula:

$$f(x,y) = \begin{cases} 255 & \text{if} \quad \mathcal{C}(x,y) > T \\ \\ 0 & \text{if} \quad \mathcal{C}(x,y) \leq T \end{cases} \tag{8}$$

where $\mathcal{C}(x,y)$ is the number of pixels that compose the connected component to which the pixel belongs (x,y) and T is a threshold.

7.7 Erosion

If A is a set representing a binary image and B is structuring element, erosion is defined for B, denoted as $A \ominus B$ [[12]]:

$$A \ominus B = \{x | x + b \in A \; for \; each \; b \in B\} \tag{9}$$

Figures 5 and 6 show the block diagram of the proposed method in its first stage.

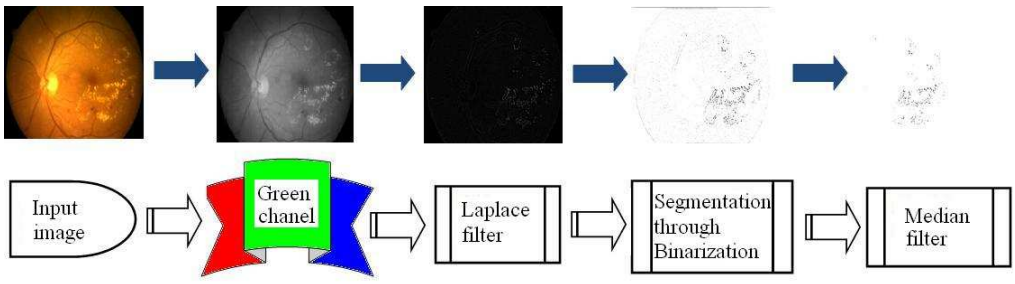

Figure 5: Block diagram of the proposed method in the first stage for obt aining the exudates.

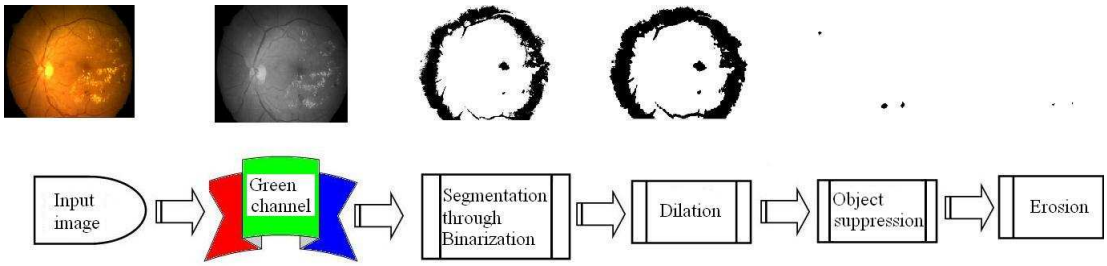

Figure 6: Block diagram of the proposed method in the first stage to obtain bleeding.

2) **feature extraction using Hu moments.** Once the segmentation of exudates and bleeding, we proceed to obtain the moments of Hu both the share of exudates as bleeding. The result are two vectors of size 7 corresponding to the 7 times of Hu, both vectors are concatenated to form a single vector of size 14 in decimal values finally this vector is binarized by Johnson-Mbius modified method [[5]] , where a pattern is obtained with a size of 14 binary values. This pattern is for the image analysis. Figure 7 shows the block diagram of the second stage.

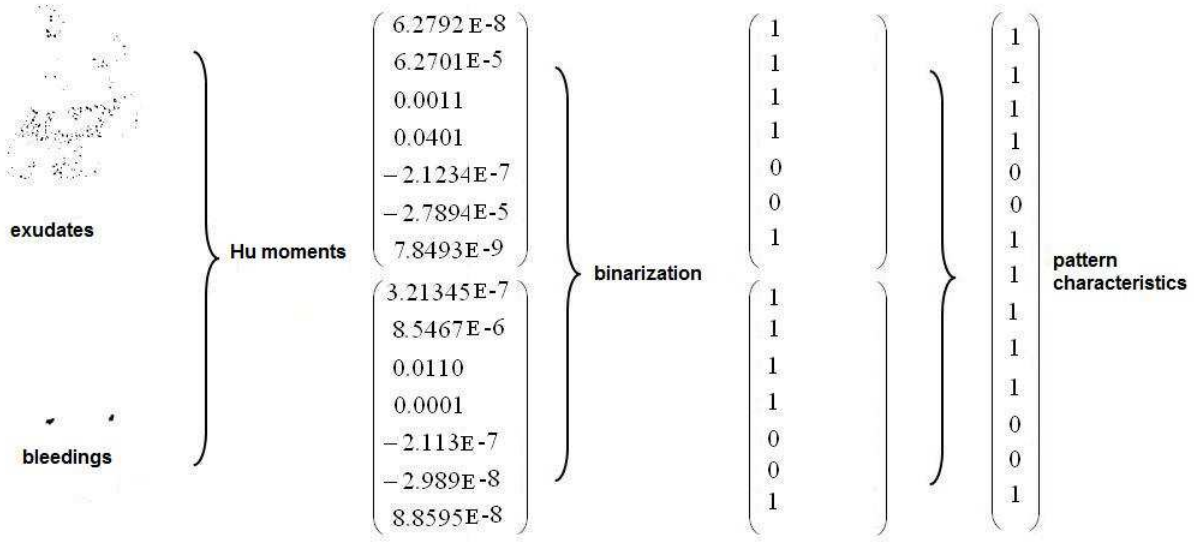

Figure 7: Second stage of the proposed method: Getting Hu moments features by.

3) **Classification using associative memories.** For the third stage, took the patterns obtained in the second stage, and used the associative memory model based on cellular automata presented in Section 6.

8. Experiments and Results

In this work we used images of the retinal vascular network of individuals extracted from a digital bank. The image bank has a repertoire of 100 images of which 60 correspond to patients suffering diabetic retinopathy and 40 without diabetes. The size of each image is 768×576 pixels. The images were obtained through the diagnostic test called angiography fluorescein that involves injecting a special dye subsequently an individual to get pictures when the dye passes through the blood vessels of the retina.

The proposed methodology was applied to each image bank images as follows: Each image is grayscale work, this was carried out by extracting only the green channel of the image. For the segmentation of exudates was applied filter Laplacian of Gaussian mask is shown in Figure 8, the image obtained was thresholds and considering the umbrals 50-200. Figure 9 shows a grayscale image and the image after applying the Gaussian filter mask proposal. For the segmentation of bleeding, considering thresholds are 55-80, for dilation and erosion structuring element was used in a cross size 5×5 and shown in Figure 10.

0	0	-1	0	0
0	-1	-2	-1	0
-1	-2	16	-2	-1
0	-1	-2	-1	0
0	0	-1	0	0

Figure 8: Mask used in the Laplacian of Gaussian.

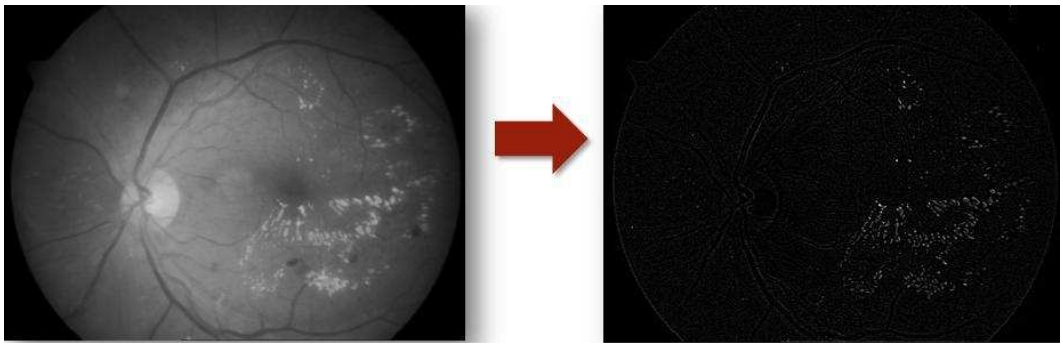

Figure 9: Image in a) is in grayscale and b) after applying the Laplacian of Gaussian mask proposal.

0	0	1	0	0
0	0	1	0	0
1	1	1	1	1
0	0	1	0	0
0	0	1	0	0

Figure 10: Structuring element used to erode and dilate.

After obtaining the results of the first stage, Hu moments applied both to the corresponding part of the exudates and of the bleeding, the result was two vectors yielded size 7, which represent the values of the seven times of Hu , these two vectors are concatenated to obtain the pattern that represents the image vector tamano getting a 14. Data were coded binary values each pattern by modified Johnson-Möbius codification of the propusal memory works with binary values. From binary patterns obtained we built and operated based associative memory cellular automata. The model was validated by cross-validation method, obtaining a yield of 95.83%.

Conclusions

In this paper presented a method for the classification of patients with diabetic retinopathy from those without diabetes. The work was divided into three stages: the collection of exudates and hemorrhages by digital image processing using spatial domain methods, obtaining the characteristics of each image using

Hu moments, and the share of classification using associative memories based on cellular automata.

Ackowledgment

The authors would like to thank the Instituto Politécnico Nacional (Secretaría Académica, COFAA, SIP, ESCOM, CIDETEC and CIC), the CONACyT and SNI for their economical support to develop this work.

References

[1] M. Aldape-Pérez, A. J. Argüelles-Cruz, O. Camacho-Nieto, C. Yáñez-Márquez, An associative memory approach to medical decision support systems. Computer Methods and Programs in Biomedicine, Volume 106, June 2012, Issue 3, Pages 287-307.

[2] A. A. Alghadyan, Diabetic retinopathy An update. Saudi Journal of Ophthalmology, Volume 25, (2011), Issue 2, Pages 99-111.

[3] E. Aptoula, S. Lefévre. A comparative study on multivariate mathematical morphology. Pattern Recognition, Volume 40, (2007), Issue 11, Pages 2914-2929.

[4] S. Barman, B. Uyyanonvara, A. Sopharak y T.H. Williamson, Automatic detection of diabetic retinopathy exudates from non-dilated retinal images using mathematical morphology methods. Computerized Medical Imaging and Graphics, Volume 32, (2008), Issue 8, Pages 720-727.

[5] O. Camacho Nieto, R. Flores Carapia, I. López Yáñez, C. Yáñez Márquez, Automatic detection of cranial fractures in radiological images using a pattern classifier. Rev. Fac. ing. univ. Antioquia. Num. 61, Diciembre 2011, pp: 29-40.

[6] D. A. Chistiakov, Diabetic retinopathy: Pathogenic mechanisms and current. Diabetes & Metabolic Syndrome: Clinical Research & Reviews, Volume 5, (2011), Issue 3, July-September 2011, Pages 165-172.

[7] J. De Lope, J. A. Martín H., M. Santos, Orthogonal variant moments features in image analysis. Volume 180, (2010),Issue 6, Pages 846-860.

[8] M. A. De Santiago, S. J. García, I. Gómez, Protocolo de Detección y Seguimiento de la Retinopatía Diabética. Medicine - Programa de Formación Médica Continuada Acreditado, ElSevier, Volume 10, (2008), Issue 17, p. 1169-1174.

[9] A. Erginay, C. Jeulin, J.-C. Klein, P. Massin, R. Ordonez, T. Walter, Automatic detection of microaneurysms in color fundus images. Medical Image Analysis, Volume 11, December 2007 (2007), Issue 6, Pages 555-566.

[10] R. Flores-Carapia, B. Luna-Benoso, C. Yáñez Márquez. Associative Memories Based on Cellular Automata: An Application to Pattern Recognition. Applied Mathematical Sciences, Vol. 7, 2013, no. 18, Pages 857 - 866.

[11] R. González, J. Woods, Digital image processing, 3rd edn. Prentice Hall, New Jersey, (2008).

[12] C. Lincke, C. A. W*ü*thrich, Surface digitizations by dilations which are tunnel-free. Volume 125, (2003), Issue 1, Pages 81-91.

[13] I. López-Yáñez, I. Román-Godínez, C. Yáñez-Márquez: Classifying Patterns in Bioinformatics Databases by Using Alpha-Beta Associative Memories. Biomedical Data and Applications. Springer. Vol 224 2009: 187-210.

[14] P. A. Mlsna, J. J. Rodríguez. Gradient and Laplacian Edge Detection. The Essential Guide to Image Processing (Second Edition), (2009), Pages 495-524.

[15] J.-F. Rivest, Morphological operators on complex signals. Volume 84, (2004), Issue 1, Pages 133-139.

[16] N. H. Solouma, D. Youssef, Accurate detection of blood vessels improves the detection of exudates in color fundus images, Computer Methods and Programs in Biomedicine, (2012)

[17] H. Sossa, R. A. Vázquez, Behavior of morphological associative memories with true-color image patterns. Neurocomputing, Volume 73, December 2009, Issues 13, Pages 225-244.

Received: October 11, 2013